이학석사 학위논문

건강 한국인 대상자에서 실로스타졸 반복 경구투여후 실로스타졸과 대사체 (OPC-13015 와 OPC-13213)의 집단 약동학 분석

Pharmacokinetic Modeling Analysis of Cilostazol and its Active Metabolites (OPC-13015 and OPC-13213) after Multiple Oral Doses of Cilostazol in Healthy Korean Volunteers

울산대학교대학원

의 학 과

최 애 령

건강 한국인 대상자에서 실로스타졸 반복 경구투여후 실로스타졸과 대사체 (OPC-13015 와 OPC-13213)의 집단 약동학 분석

지 도 교 수　　임 형 석

이 논문을 이학석사 학위 논문으로 제출함

2018 년 12 월

울 산 대 학 교 대 학 원
의　학　과
최　애　령

최애령의 이학석사학위 논문을 인준함

심사위원	노규정	(인)
심사위원	임형석	(인)
심사위원	김상엽	(인)

울 산 대 학 교 대 학 원
2018 년 12 월

국문요약

연구목적: 실로 스타 졸은 PDE3 (phosphodiesterase type III)의 선택적 억제제로서 간헐적인 파행 (intermittent claudication)이 있는 말초 혈관 질환에 사용된다. 본 연구의 주요 목적은 건강한 한국인 자원자들에서 실로스타졸 프레탈 정제의 식후 반복 투여 시 cilostazol 과 그 활성 대사체 (OPC-13015, OPC-13213)의 집단 약동학을 탐색하는 것이다.

연구방법: 건강 자원자 24 명을 대상으로 2x2 교차설계 임상시험이 수행하여 실로스타졸 서방형 캡슐 제제와 프레탈® 정제의 식후 반복 투여하였다. 각 자원자에서 지정된 시간에 따라 채혈이 진행되었고 그 중 프레탈® 정제를 복용한 후 측정된 실로스타졸 및 그 활성대사체의 혈중 농도 데이터만 사용하여 순차적 접근법으로 비선형혼합효과모형 분석 (NONMEM® 7.4)을 진행하였다.

결과: 실로스타졸의 시간-혈중 약물 농도는 1 차 구획 모델에 의해 가장 잘 묘사되었고 흡수 초기에 시간 지연이 있는 0 차 및 1 차 속도 혼합 흡수 모델이 적용되었다. D1 (0 차 흡수 지속 시간), Ka (1 차 흡수 속도 상수) 및 F1 (상대적 생체 이용률)에 투약간 변이(interoccasional variability)를 도입하여 모델 적합성이 크게 개선되었고 체수분량 (Total body water)이 클리어런스에 영향 주는 유의미한 공변량으로 확인되었다.

결론: 본 연구에서 제시한 PK 모델은 한국 남성 자원자에서 cilostazol 의 PK 특성을 탐구하였고 약물의 최적의 개별 투여 요법을 확인하는 데 유용할 수 있을것이다.

Contents

List of Tables and Figures

INTRODUCTION

Cilostazol (6-[4-(1-cyclohexyl-1*H*- tetrazol-5-yl)butoxy]-3,4-dihydro-2(1*H*)-quinolinone) is a quinolinone derivative, and several of its metabolites selectively inhibit cellular phosphodiesterase III (PDE III) and adenosine uptake, which inhibit degradation of intracellular 3′,5′-cyclic adenosine monophosphate in platelets and blood vessels, leading to symptomatic effects on antiplatelet aggregation and vasodilation.[1-3]

Cilostazol also exhibits antiproliferative effects on smooth muscle cells and has favorable influences on high-density lipoprotein cholesterol and triglyceride levels. It is approved to treat the intermittent claudication symptoms caused by peripheral arterial disease. Cilostazol also significantly reduces recurrent ischemic stroke and hemorrhagic events and effectively prevents cerebral infarction[4-5]. In addition, it can reduce the growth of carotid intima-media thickness in diabetic patients[6]. However, despite these potential benefits of cilostazol, some patients have discontinued treatment due to undesirable side effects such as headache, palpitation, and diarrhea[1].

Cilostazol shows appreciable inter-individual variation in bioavailability, and the coefficient of variation in most of these pharmacokinetic (PK) parameters of cilostazol ranges from 40% to 60%[7]. Cilostazol is extensively metabolized to dehydrocilostazol (OPC-13015) and monohydroxy-cilostazol (OPC-13213) via CYP3A5 and CYP2C19, respectively[8-9]. For inhibitory effects on platelet aggregation, OPC-13015 is 3–7 times more potent than cilostazol, whereas OPC-13213 is one-third to one-fifth times less potent than plasma cilostazol. During evaluation of cilostazol, it is important to take into account the pharmacological effects of the primary metabolite OPC-13015, as it is 15% of the total oral administered radiolabeled cilostazol.

The objective of this study was to assess the PK properties of cilostazol and its two active metabolites, and to detect significant covariates (COVs) that might introduce variability in exposure after oral administration. In addition, to reduce the rate of adverse effects, information is provided

to aid in enhancing the prediction of appropriate dose adjustments of cilostazol based on the PK parameters of additional metabolites and its significant COVs.

Methods

Clinical Pharmacokinetic Data of Cilostazol and its Active Metabolites

The PK dataset used in this analysis was collected from a phase I study comparing the PK of immediate (IR) and sustained release (SR) formulations of cilostazol conducted at the Department of Clinical Pharmacology and Therapeutics in Asan Medical Center (Seoul, Republic of Korea)[10]. In this randomized, open-label, multiple-dose clinical trial in healthy Korean adult males, 30 subjects were randomly assigned to two sequence groups that consisted of two treatment groups of IR (100 mg cilostazol IR, every 12 h for 5 days) and SR (200 mg cilostazol SR, every 24 h for 5 days) interspersed with a 9-day washout period. Of the 30 enrolled healthy Korean male participants, 24 completed all study procedures (12 in each sequence) and 6 participants withdrew (5 withdrawals were due to adverse effects [headache] and 1 withdrawal was for personal reasons). Only PK data on the IR formulation were used in this analysis. For the analysis, blood was drawn in a sodium heparin-coated tube immediately before and at 1, 2, 4, 6, 8, 10, 12, 24, 48, 72, 96 (pre-dose level on day 5), 97, 98, 99, 100, 102, 104, 106, 108, 112, 120, 132, 144, and 168 h after the first dose of IR formulation. Blood samples were immediately placed in an ice bath. Plasma was separated by centrifugation at 1,800×g for 10 min at 4°C and stored at -20°C until analysis. A validated liquid chromatography-tandem mass spectrometry (LC-MS/MS) method to simultaneously measure cilostazol and its active metabolites (OPC-13015 and OPC-13213) in human plasma was used based on previous reports. Cilostazol and the internal standard, mosapride, were separated using a high-performance liquid chromatography system (Spark Holland, Emmen, The Netherlands) and detected by MS/MS (API 4000; Applied Biosystems/MDS Sciex, Toronto, Canada). The lower limit of quantification was 0.5 ng/mL, with the calibration curve ranging from 0.5 ng/mL to 2,000 ng/mL. Finally, respective 768 cilostazol, OPC-13015, and OPC-13213 concentrations were used in the PK modeling analysis. The volunteer characteristics included in

this analysis are summarized in Table 1.

Feature	Mean (s.d.)	Range	
AGE, year	27.9 (6.1)	22.0	49.0
WT, kg	69.5 (6.2)	58.5	83.0
HT, cm	173.1 (6.0)	164.2	186.6
BMI, kg/m^2	23.2 (2.0)	18.6	26.5
BFM, lbs	13.1 (3.5)	6.1	22.0
FFM, lbs	56.6 (5.8)	46.6	66.8
TBW, lbs	42.4 (5.6)	34.2	60.1
SLM, lbs	53.5 (5.5)	43.9	63.0
SMM, lbs	32.0 (3.5)	25.7	38.0
VFA, cm^2	62.1 (21.2)	14.4	107.3
ICW, lbs	26.0 (2.7)	21.3	30.6
ECW, lbs	15.6 (1.5)	12.9	18.4

Table 1 Demographics and baseline information of healthy volunteers (n=24) included in this analysis. Abbreviations: AGE, age; WT, weight; HT, height; BMI, body mass index; BFM, body fat mass; FFM, fat free mass; TBW, total body water; SLM, soft lean mass; SMM, keletal muscle mass; VFA, visceral fat area; ICW, intracellular water; ECW, extracellular water

Modeling Strategy

The plasma molar concentrations of cilostazol and its active metabolites over time were analyzed by Nonlinear Mixed Effects Modeling (NONMEM) using NONMEM software version 7.4 (Icon Development Solutions, Ellicott City, MD, USA). ADVAN13 subroutine and the first-order conditional estimation method in NONMEM were used for the estimation. Parent and metabolite PK analysis was conducted sequentially, in which the volume of distribution (V_d) for OPC-13015 and OPC-13213 was fixed at the typical values (V_d) for cilostazol due to an identifiability problem[11]. Cilostazol PK was modeled first, and then the concentration of its metabolites, OPC-13015 and OPC-13213, were fit simultaneously with cilostazol concentrations after fixing the initial values of fixed and random-effects parameters for cilostazol PK at the final estimates of the previous run for cilostazol only. For more detail, the inter-individual variability (IIV) of each parameter of the basic

model was modeled using the following exponential error model:

$$\mathrm{Pi} = P_{TV} \cdot \exp(\eta \mathrm{i}) \quad (1)$$

where P_i is the value of the parameter in the i^{th} individual, η_i is a random variable and the difference between P_i and P_{TV}, which is the value of the parameter in a typical individual. It is assumed that the values of η_i are normally distributed with a mean of zero and a variance of ω^2. A proportional error model as following equation was used to describe the residual variability after testing of various residual models:

$$C_{obs,ij} = C_{pred,ij} \cdot (1 + \varepsilon_{pro,ij}) \quad (2)$$

where $C_{obs,ij}$ is the j^{th} observed value in the i^{th} volunteer, $C_{pred,ij}$ is the j^{th} predicted value in the i^{th} volunteer, and $\varepsilon_{pro,ij}$ is the residual variability with means of zero and variances of σ^2. The correlation between IIVs in the model was explored using the OMEGA BLOCK option if possible. Various compartment models for cilostazol (parent) and two metabolites were tested. For cilostazol, various absorption models, such as first-order (Ka) and zero-order (D1), Weibull, IIV in relative bioavailability (F1), lag time at the beginning of absorption (ALAG1), and transit compartment model were evaluated.

Inter-occasional variabilities (IOVs) were also implemented for various PK parameters based on the drug administration times as follows:

$$\eta = \eta\mathrm{IIV} + (\eta\mathrm{IOV1} + \eta\mathrm{IOV2} + \eta\mathrm{IOV3} + \eta\mathrm{IOV4}) \quad (3)$$

where η is a realized value from unexplained IIV and unexplained IOV; η_{IIV} is a realized IIV from random variable for unexplained IIV; η_{IOVn} is a realized IIV from random variable for unexplained IOV, and ns are 1, 2, 3, 4. In the metabolites PK model for OPC-13015 and OPC-13213, the total clearance (CL) of cilostazol was divided into three parts (OPC-13015, OPC-13213, other) in which the fractions of total CL of cilostazol into the two metabolites were described as following logistic models to confine the metabolic fractions (FM1 and FM2) between 0 and 1:

$$\mathrm{FM1} = \exp(\mathrm{FM1F})/(1 + \exp(\mathrm{FM1F}) + \exp(\mathrm{FM2F})) \quad (4)$$

$$\mathrm{FM2} = \exp(\mathrm{FM2F})/(1 + \exp(\mathrm{FM1F}) + \exp(\mathrm{FM2F})) \quad (5)$$

$$\mathrm{OTHER\ CL} = 1/(1 + \exp(\mathrm{FM1F}) + \exp(\mathrm{FM2F})) \quad (6)$$

In these equations, FM1 and FM2 are the fractions of CL of cilostazol (parent) into OPC-13015 and OPC-13213, respectively, which are described by factors comprising the logistic model (FM1F, FM2F). The Other CL is the fraction of cilostazol CL other than OPC-13015 and OPC-13213. Here, FM1F and FM2F were estimated in this analysis and their unexplained IIV was modeled using the following additive model:

$$P_i = P_{TV} + \eta_i \quad (7)$$

where P_i is the value of a parameter for the i^{th} individual, P_{TV} is the typical population parameter value, and η_i is a random variable reflecting unexplainable IIVs with a mean of 0 and a variance of ω^2.

Covariate screening

Several demographic factors were tested as potential COVs for the PK model, such as age, weight, height, body mass index, body fat mass, fat free mass, total body water (TBW), soft lean mass, skeletal muscle mass, visceral fat area, intracellular water, and extracellular water (Table 2). A power model that centered the COV to its mean values was applied to allow greater flexibility in the relationship between the parameter and the COV.

$$P_i = \theta_1 \times \left(\frac{\mathrm{COV_i}}{\mathrm{mean\ COV}}\right)^{\theta_2} \quad (8),$$

where P_i is the value of a parameter in the i^{th} individual, θ_1 and θ_2 are the typical parameter values to be estimated, θ_1 is the typical parameter estimate for a volunteer with mean COV value; θ_2 is the exponent in the power model; and COV_i is the COV of the i^{th} volunteer; mean COV is the calculated

mean COV from all of the volunteers. To confirm the statistical significance of the COVs included in the final model, randomization tests with 1,000 sample datasets were performed[12].

Model evaluation

The statistical significance of each COV in the PK models was tested individually in NONMEM. A full model was built by stepwise additions of each significant COV, and then each COV was eliminated to obtain the final model. The likelihood ratio test was used for hypothesis testing to discriminate among alternative hierarchical models, with strict inclusion significance at 0.01, and exclusion significance at 0.005, which corresponds to a decrease in objective function value (OFV) of 6.63 and 7.88, respectively. After initial univariate analyses were completed, the COV producing the most significant decrease in OFV was included in the new COV model, which was repeated until there were no further COVs that caused a significant decrease in the OFV. The resulting model was considered the full model. If more than two COVs were included in the full model, backward elimination was employed, during which each COV was removed from the model separately. The backward elimination procedure was repeated until all of the remaining COVs were significant. The COV screening was conducted in respective parent and metabolite PK modeling.

RESULTS

The plasma cilostazol concentration over time was best fit by the one-compartment linear disposition model. The absorption properties were described by mixed zero (D1)- and first-order kinetics with lag time (ALAG1) in NONMEM, in which inclusion of IIV for relative bioavailability (F1), and inter-occasional variabilities in Ka, D1, and F1 significantly improved the model fit based on diagnostic plots and the decrease in OFV.

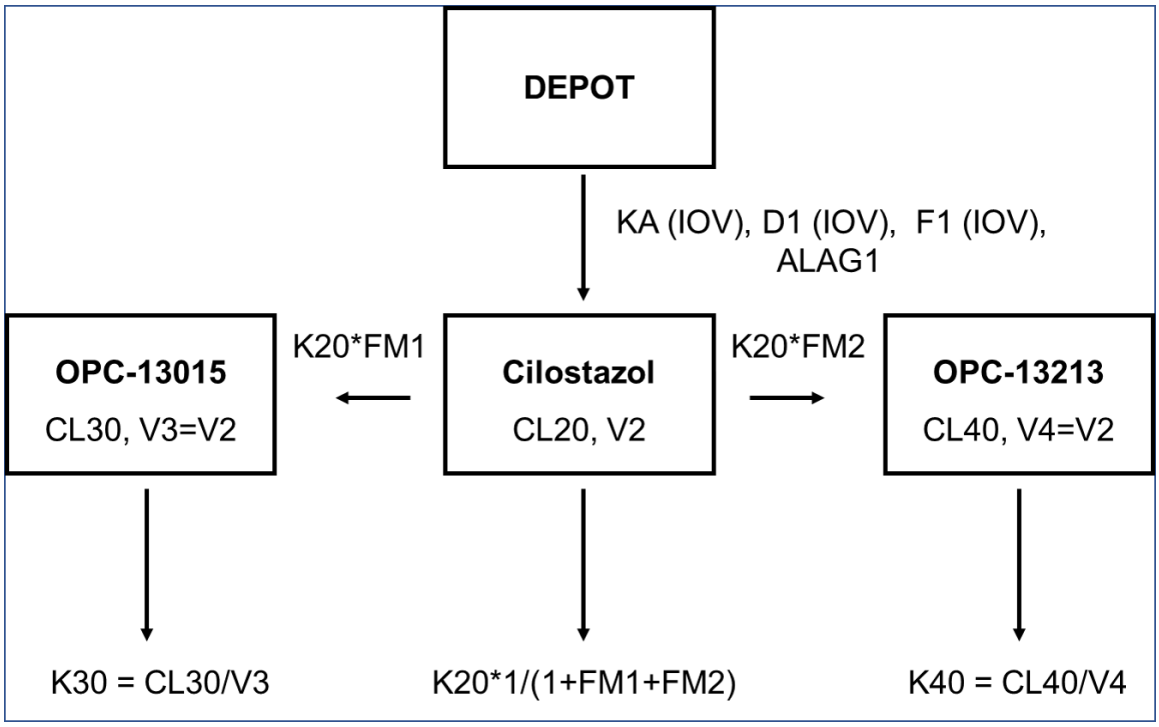

Figure 1 Population pharmacokinetic model structure for cilostazol and its active metabolites.
Abbreviations: K20, elimination rate constant for cilostazol; CL20, total clearance for cilostazol; V2, volume of distribution for cilostazol; V3 and V4 are fixed at the typical value of volume of distribution for cilostazol due to identifiability problem; K30, elimination rate constant for OPC-13015; CL30, clearance for OPC13015; K40, elimination rate constant for OPC13213; CL40, clearance for OPC13213; FM1=exp(FM1F)/ (1+exp(FM1F)+exp(FM2F)), the fraction of clearance of cilostazol converted into OPC-13015; FM2=exp(FM2F)/(1+exp(FM1F)+exp(FM2F)), the fraction of cleaarance of cilostazol converted into OPC-13213.

TBW was identified as the only COV affecting the clearance of cilostazol. The inclusion of TBW in the clearance of cilostazol in the form of power function significantly decreased the OFV (Model 4 in Table 2), with the exponent estimated as 1.33.

Table 2 Pharmacokinetic models of cilostazol tested in this study

Model	Dataset used	Model description	OFV
Model 1	Plasma cilostazol	1-compartment with first-order absorption	260
Model 2	Plasma cilostazol	1-compartment with zero- and first-order absorption, D1, ALAG1	41
Model 3	Plasma cilostazol	1-compartment with zero- and first-order absorption ALAG1 and IOV in KA, D1, F1	-216
Model 4	Plasma cilostazol	Model 3 with TBW on clearance	-232

Abbreviations: Ka, first-order absorption rate constant; D1, duration of first-order input; ALAG1, lag time in the beginning of the absorption; F1, relative bioavailability.

The PK of both metabolites (OPC-13015, OPC-13213) was described by a one compartment linear model. The population parameter estimates of the final model are shown in Table 3. Standard errors of most parameter estimates were in acceptable ranges, with the exception of the IIV of the Vd and IIV of ALAG1 without bias. Although they showed large standard errors resulting in a wide 95% confidence interval (CI) inclusive of 0, they were still regarded as statistically significant because the OFV changes were significant based on our modeling evaluation criteria. Proportional error model fit the parent data most, whereas combined error model fit both metabolites.

Table 3 Population pharmacokinetic parameter estimates of cilostazol in healthy Korean participants.

Parameter		Estimates	RSE%	95% CI	Bootstrap	
					Median	95% CI
Cilostazol	CL	7.17	7%	6.13~8.21	6.941	6.31~7.93
(parent drug)	IIV_{CL} (CV, %)	0.03 (62%)	29%	0.02~0.05	0.05	0.02~0.11
	V	9.39	18%	6.12~12.66	8.196	6.66~9.86
	IIV_{V} (CV, %)	0.09 (63%)	88%	-0.06~0.24	0.07	0.02~0.26
	Ka	0.16	7%	0.14~0.18	0.153	0.14~0.17
	IOV_{Ka} (CV, %)	0.08 (63%)	39%	0.02~0.15	0.08	0.05~0.15
	D1	2.37	12%	1.80~2.94	2.606	2.23~3.43
	IOV_{D1} (CV, %)	0.77 (89%)	25%	0.39~1.15	0.6	0.28~1.00
	ALAG1	0.22	42%	0.04~0.41	0.219	0.09~0.32
	IIV_{ALAG1} (CV, %)	0.35 (72%)	113%	-0.43~1.14	0.18	0.03~1.31
	IOV_{F1} (CV, %)	0.13 (65%)	13%	0.10~0.17	0.12	0.03~0.26
	ε (addictive)	0.000001 FIX				
	ε (proportional)	0.26	3%	0.24~0.27	0.255	0.21~0.27
	θ_{CL} for TBW	1.42	49%	0.07~2.77	1.408	0.10~3.12
OPC-13015	CL	2.02	7%	1.73~2.31	2.09	1.71~2.51
	IIV_{CL} (CV, %)	0.13 (65%)	56%	-0.01~0.27	0.12	0.06~0.19
	FM1F	-2.27	-7%	-2.56~-1.98	-2.28	-2.46~-2.09
	IIV_{FM1F} (CV, %)	0.10 (64%)	35%	0.03~0.18	0.08	0.01~0.14
	ε (addictive)	0.01	13%	0.01~0.01	0.01	0.00~0.02
	ε (proportional)	0.12	4%	0.11~0.13	0.12	0.09~0.16
OPC-13213	CL	6.15	12%	4.69~7.61	6.23	5.59~7.04
	IIV_{CL} (CV, %)	0.04 (62%)	38%	0.01~0.07	0.03	0.00~0.06
	FM2F	-2.46	-7%	-2.80~-2.12	-2.46	-2.69~-2.25
	IIV_{FM2F} (CV, %)	0.11 (64%)	56%	-0.01~0.22	0.09	0.03~0.17
	ε (addictive)	0.01	13%	0.01~0.01	0.01	0.01~0.01
	ε (proportional)	0.14	6%	0.13~0.16	0.15	0.12~0.20

Abbreviations: RSE, relative standard error (standard error divided by the parameter estimate); IIV, inter-individual variability; variance (% coefficient of variation (CV), calculated by CV (%) = sqrt (exp (omega) −1)) × 100; V, typical volume of distribution; CL, typical clearance; Ka, typical absorption rate constant; D1, duration time; ALAG1, lag time; Θ_{CL} for TBW represents the covariate effect of total body water (TBW) centralized to 40L on the CL expressed as a power function in the form of Eq. 8 where CL is a typical CL in participants; ε (addictive) is represented as the standard deviation, ε (proportional) is represented as the standard deviation; FM1F, value that determines the fraction of cilostazol clearance convert into OPC-13015 in logit model (Eq. 4); FM2F, value that determines the fraction of cilostazol clearance convert into OPC-13213 in logit model (Eq. 5)

The total CL of cilostazol was estimated to be 7.17 L/h and the fractions of total cilostazol CL converted to OPC-13015 and OPC-13213 were calculated as 8.69% (0.62 L/h) and 7.19% (0.52 L/h), respectively, under the assumption that the individual Vd of the two metabolites was the same as the typical Vd of the parent compound. The respective total CLs of OPC-13015 and OPC-13213

were estimated to be 2.02 L/h and 6.15 L/h. In randomization tests, the TBW on total CL of cilostazol was confirmed to be statistically significant (p=0.005), as the OFV of the final model was much lower than the 2.5 percentile of the OFV distribution obtained from 1,000 replicates of NONMEM runs based on the datasets, in which the TBW was randomly permuted over the individual subjects (Fig. 5)[13].

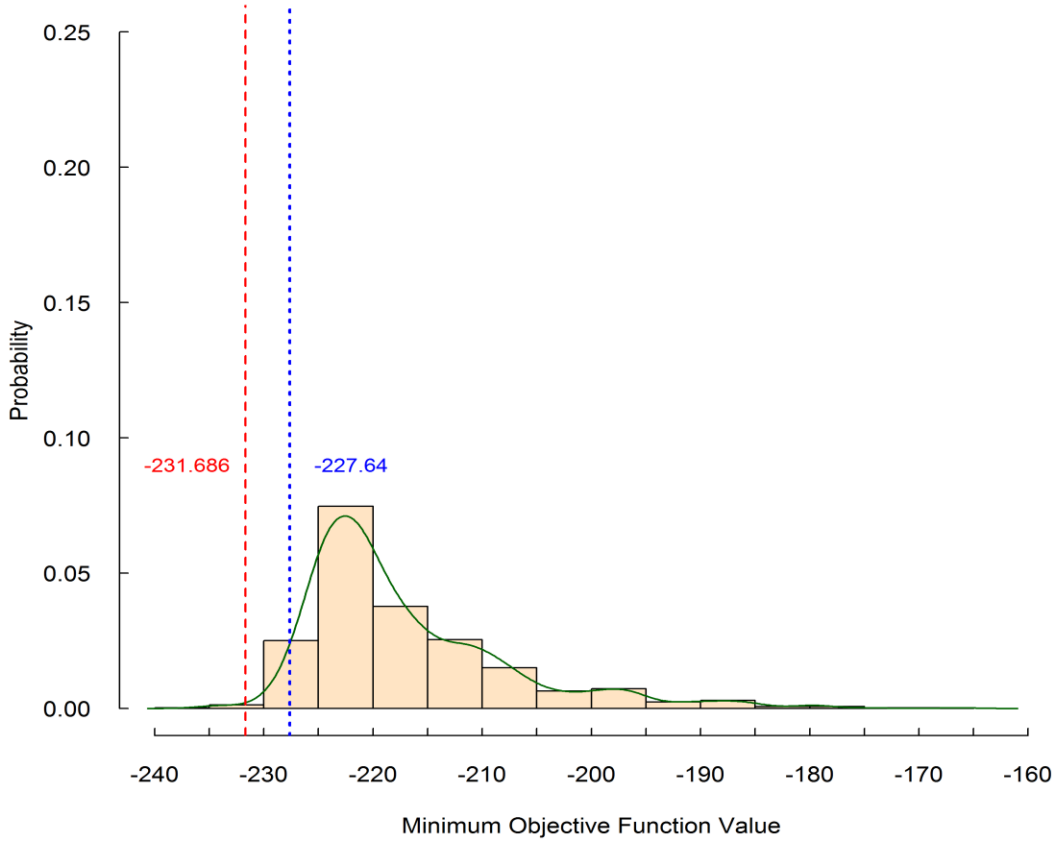

Figure 2 Randomized test for the effect of TBW on Cilostazol clearance.

DISCUSSION

In this study, a PK model for cilostazol and its two active metabolites (OPC-13015 and OPC-13213) were successfully constructed, in which the PK of cilostazol was best described by a one-compartment model with mixed zero- and first-order kinetics and lag time in absorption process, and those of OPC-13015 and OPC-13213 were best depicted by one compartment model. This is the first analysis describing the population PK of cilostazol together with its two active metabolites after multiple oral administrations of cilostazol IR formulation in healthy Korean male volunteers.

Overall, the absorption process of an orally administrated drug is complicated, and is affected by drug-specific and patient-specific characteristics. An inappropriate absorption model could result in the biased estimation of disposition PK parameters such as the Vd and CL. Taking into consideration the complexity of the absorption properties, we applied various absorption models to explain the large IIV in the absorption-related parameters, including zero-, first-, mixed zero- and first-order absorption models, the Weibull model, the transit absorption compartment model, and their combinations. Ultimately, the mixed zero- and first-order absorption models with lag time and inclusion of IIV in relative bioavailability (F1) were the best absorption models given the available concentration data. Introduction of IOV to D1, Ka, F1, further improved the model fit, with an obvious decrease in OFV and IIVs of the corresponding parameters as shown in Tables 2 and 3.

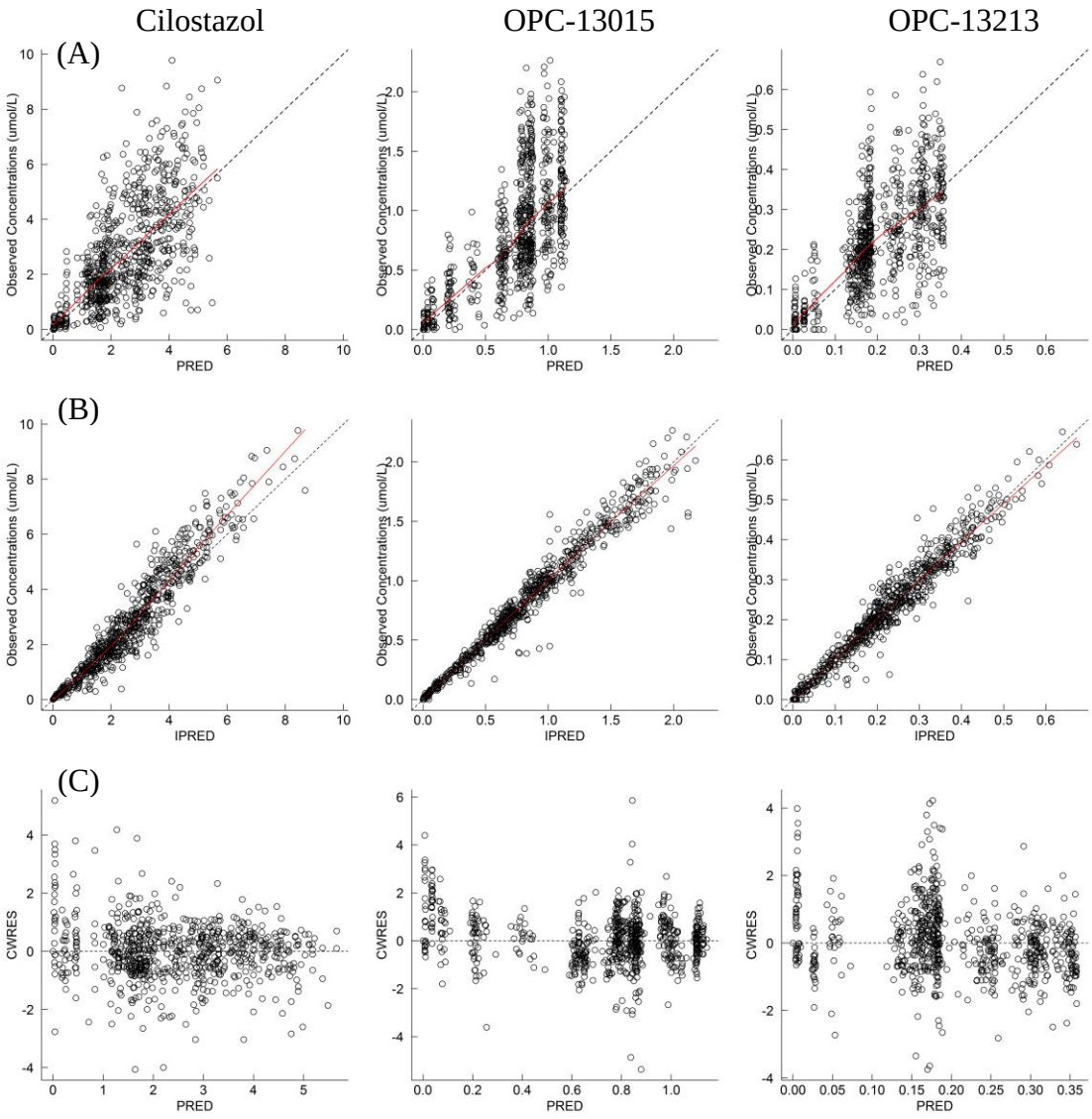

Figure 3 Goodness of fit plots for the final population pharmacokinetics (PK) model.
Abbreviations: PRED, population predicted concentrations; IPRED, individual predicted concentrations; CWRES, conditional weighted residuals (A) Plot of observed cilostazol and OPC-13015 and OPC-13213 concentrations versus population predicted concentrations. Black dash line, line of identity; red line, data smoother. (B) Plot of observations versus individual predictions. Black dash line, line of identity; red line, data smoother. (C) Plot of population CWRES versus population predictions. Black dash line, zero-slope line; red line, data smoother.

The scatter plot of observation versus prediction based on the final PK model showed that the points were tightly clustered around the line without systematic bias across the range of measured values (Fig. 2). In the dpendent variable (DV) versus individual prediction (IPRED) plot,

there was a significant improvement after inclusion of IOVs in the absorption-related parameters. Conditional weighted residuals of the final model showed symmetric distribution around the reference line without any noticeable trend, and most residuals were within the range of −1.96 through 1.96, which suggests that our model described cilostazol PK well. The concentration over time plots showed good concordance between the observed and predicted concentrations. These results indicate the qualified stability of the final model and support the reliability of the parameter estimates. The VPC plots of cilostazol and OPC-13015 and OPC-13213 were performed by simulating with 1000 replicates using the final model to assess the predictive performance. As depicted in Figure 3, most the observed concentrations were equally distributed in the median prediction lines and were within a 90% prediction interval based on simulations from the final model, although slight overprediction for cilostazol was observed during the absorption phase. Median and 95% CIs for the PK parameter estimates from non-parametric bootstrap analysis with 1,000 replicates showed similar results with those from single NONMEM run (Table 3).

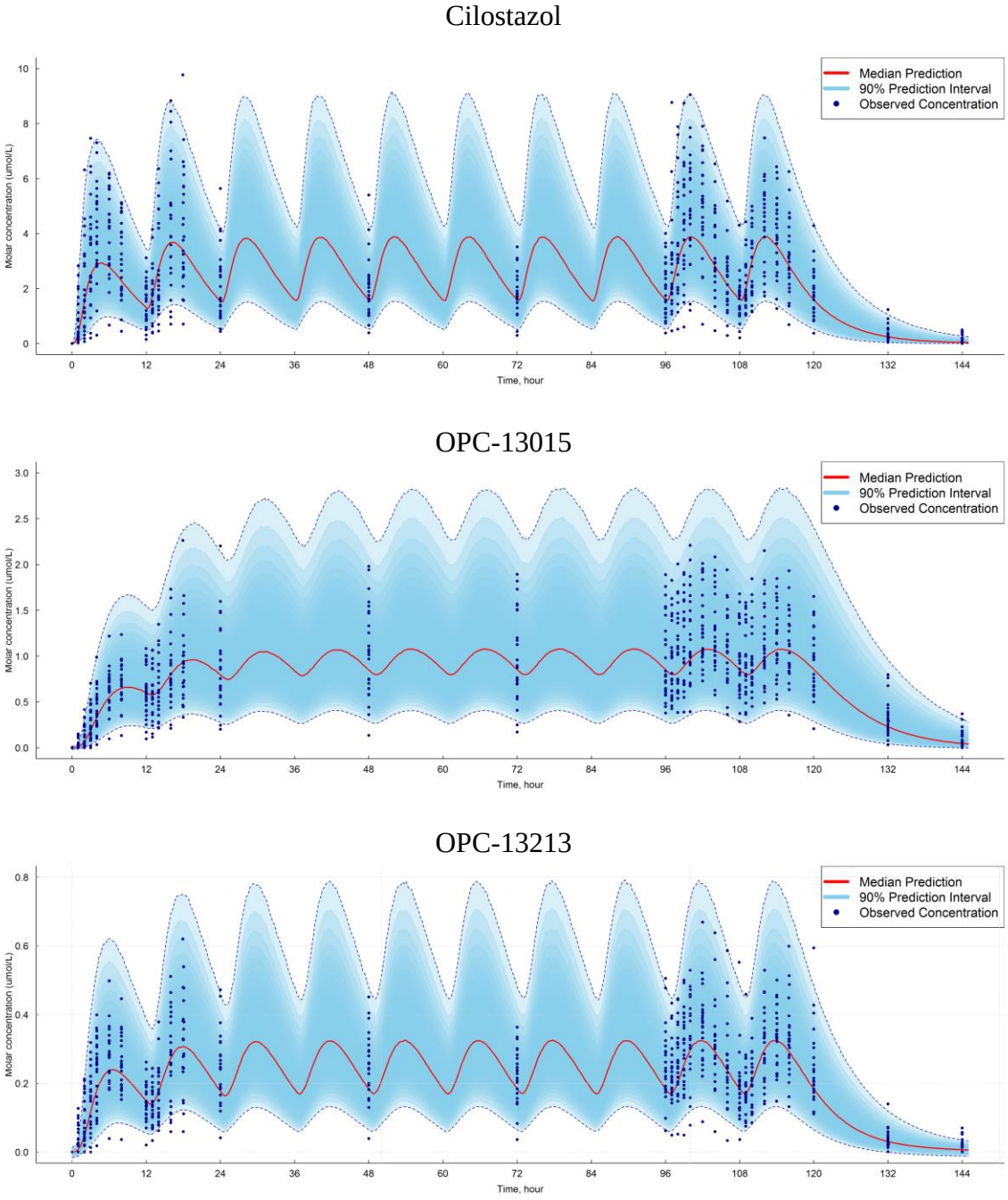

Figure 4 Visual Predicted Check (VPC) plots for the final population PK model.
Upper panel is the VPC of plasma cilostazol; middle panel is the VPC of plasma OPC-13015; lower panel is the VPC of plasma OPC-13213. In each plot, the solid red line represents the median predicted plasma concentration and the semitransparent field represents a simulation-based 90% confidence interval. Observed and predicted concentrations are in micromole per liter; Time is in hours.

Cilostazol is biotransformed to OPC-13015 and OPC-13213 via CYP3A5 and CYP2C19,

respectively[14]. The fractions of total cilostazol CL that was converted into OPC-13015, OPC-13213, and the Other pathway were estimated using the logistic model (Eqs. 4, 5, 6) taking the IIV of the fraction into account. The estimated conversion fractions of OPC-13015 and OPC13213 were 8.69% and 7.19%, respectively (Table 3). However, these fractions are the only ones estimated under the assumption that the Vd for OPC-13015 and OPC-13213 are the same as the typical Vd for cilostazol. The Vds for the two metabolites were fixed at the typical Vd for cilostazol due to identifiability problems in the parent-metabolite modeling[1]. The CLs of OPC-13015 and OPC-13213 were estimated to be 2.02 L/h and 6.15 h/L, respectively. We generally individualized existing treatments based on weight and body surface area, which has sometimes been shown to be inadequate in body composition studies. For example, doses based on PK data obtained in normal body weight individuals can induce errors in drug prescriptions in obese patients[15]. For lipophilic drugs, Vd correlates better with body fat mass than total body weight. In this study, we found that TBW has a positive correlation with the total CL of cilostazol with the estimate of the exponent in the power model is 1.42. However, it is difficult to provide physiological explanations for the positive relationship between TBW and CL of cilostazol, which is a lipophilic drug of octanol-water partition coefficient of 570 (at pH 7.0)[16]. There was also a limitation in the study design, as only subjects with homogeneous demographic characteristics were enrolled in this study, which made it difficult to evaluate the effects of potential COV for the PK.

To evaluate the quantitative effects of TBW on the PK, we performed sensitivity analysis, where simulation for the plasma cilostazol concentration over time profiles was conducted at each of extreme cases for TBW (the lowest and highest). The PK profiles for the two extreme cases were not so similar with each other, which suggests that TBW might have actual clinical significance.

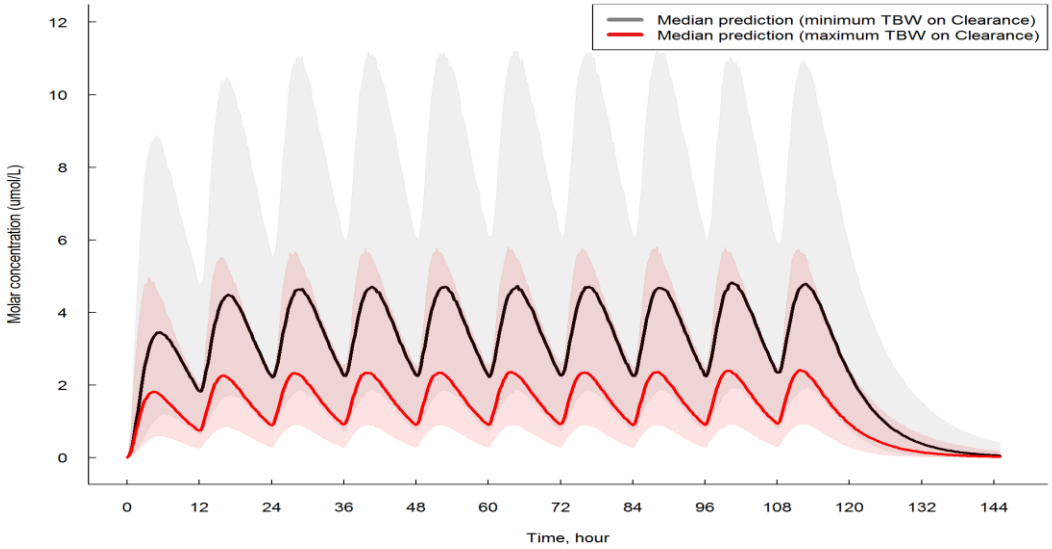

Figure 5 Sensitivity analysis of covariate TBW on cilostazol clearance.
TBW, total body water; Minimum value of TBW is 34.2 lbs; Maximum value of TBW is 60.1 lbs.

CONCLUSION

In this study, we developed PK models for cilostazol and its active metabolites (OPC-13015 and OPC-13213) after multiple oral administrations of the IR formulation of cilostazol in healthy Korean male subjects. TBW was identified quantitatively as a COV affecting the clearance of cilostazol. The current model will be useful for understanding the PK properties of cilostazol and metabolites, and for developing individualized cilostazol therapy through which the therapeutic effectiveness can be maximized, while minimizing adverse drug reactions such as headache.

REFRENCES

1. Liu, Y.; Shakur, Y.; Yoshitake, M.; Kambayashi, J. i., Cilostazol (Pletal®): a dual i nhibitor of cyclic nucleotide phosphodiesterase type 3 and adenosine uptake. *Cardiovascu lar drug reviews* **2001,** *19* (4), 369-386.
2. Kimura, Y.; Tani, T.; Kanbe, T.; Watanabe, K., Effect of cilostazol on platelet aggr egation and experimental thrombosis. *Arzneimittel-Forschung* **1985,** *35* (7A), 1144-1149.
3. Kambayashi, J.; Liu, Y.; Sun, B.; Shakur, Y.; Yoshitake, M.; Czerwiec, F., Cilostaz ol as a unique antithrombotic agent. *Current pharmaceutical design* **2003,** *9* (28), 2289-23 02.
4. Robless, P.; Mikhailidis, D. P.; Stansby, G. P., Cilostazol for peripheral arterial dis ease. *Cochrane database of systematic reviews* **2007,** (1).
5. Liu, Y.; Fong, M.; Cone, J.; Wang, S.; Yoshitake, M.; Kambayashi, J.-i., Inhibition of adenosine uptake and augmentation of ischemia-induced increase of interstitial adenos ine by cilostazol, an agent to treat intermittent claudication. *Journal of cardiovascular ph armacology* **2000,** *36* (3), 351-360.
6. Matsuda, N.; Naraoka, M.; Ohkuma, H.; Shimamura, N.; Ito, K.; Asano, K.; Hase gawa, S.; Takemura, A., Effect of cilostazol on cerebral vasospasm and outcome in patien ts with aneurysmal subarachnoid hemorrhage: a randomized, double-blind, placebo-contr olled trial. *Cerebrovascular Diseases* **2016,** *42* (1-2), 97-105.
7. Mohr, J.; Thompson, J.; Lazar, R. M.; Levin, B.; Sacco, R.; Furie, K.; Kistler, J.; A lbers, G.; Pettigrew, L.; Adams Jr, H., A comparison of warfarin and aspirin for the preven tion of recurrent ischemic stroke. *New England Journal of Medicine* **2001,** *345* (20), 1444 -1451.
8. Kwon, S. U.; Cho, Y.-J.; Koo, J.-S.; Bae, H.-J.; Lee, Y.-S.; Hong, K.-S.; Lee, J. H.; Kim, J. S., Cilostazol prevents the progression of the symptomatic intracranial arterial ste nosis: the multicenter double-blind placebo-controlled trial of cilostazol in symptomatic i ntracranial arterial stenosis. *Stroke* **2005,** *36* (4), 782-786.
9. Bramer, S. L.; Forbes, W. P.; Mallikaarjun, S., Cilostazol pharmacokinetics after si ngle and multiple oral doses in healthy males and patients with intermittent claudication r esulting from peripheral arterial disease. *Clinical pharmacokinetics* **1999,** *37* (2), 1-11.
10. Kim, Y. H.; Ghim, J.-L.; Jung, J. A.; Cho, S.-H.; Choe, S.; Choi, H. Y.; Bae, K.-S.; Lim, H.-S., Pharmacokinetic comparison of sustained-and immediate-release formulation s of cilostazol after multiple oral doses in fed healthy male Korean volunteers. *Drug desig n, development and therapy* **2015,** *9*, 3571.
11. Zhang, L.; Beal, S. L.; Sheiner, L. B., Simultaneous vs. sequential analysis for pop ulation PK/PD data I: best-case performance. *Journal of pharmacokinetics and pharmaco dynamics* **2003,** *30* (6), 387-404.
12. Abbas, R.; Chow, C.; Browder, N.; Thacker, D.; Bramer, S.; Fu, C.; Forbes, W.; O domi, M.; Flockhart, D., In vitro metabolism and interaction of cilostazol with human hep atic cytochrome P450 isoforms. *Human & experimental toxicology* **2000,** *19* (3), 178-184.
13. Holford, N.; Hashimoto, Y.; Sheiner, L. B., Time and theophylline concentration h elp explain the recovery of peak flow following acute airways obstruction. *Clinical pharm acokinetics* **1993,** *25* (6), 506-515.
14. Akiyama, H.; Kudo, S.; Shimizu, T., The metabolism of a new antithrombotic and

vasodilating agent, cilostazol, in rat, dog and man. *Arzneimittel-Forschung* **1985,** *35* (7A), 1133-1140.
15. Cheymol, G., Clinical pharmacokinetics of drugs in obesity. *Clinical pharmacokinetics* **1993,** *25* (2), 103-114.
16. Morgan, D. J.; Bray, K. M., Lean body mass as a predictor of drug dosage. *Clinical pharmacokinetics* **1994,** *26* (4), 292-307.

영문요약

Cilostazol is a selective inhibitor of phosphodiesterase type III (PDE3), which is prescribed for patients with peripheral arterial disease, especially intermittent claudication. The purpose of the study was to investigate the pharmacokinetics (PK) of cilostazol and its metabolites (OPC-13015, OPC-13213) on the immediate release (IR) formulation of cilostazol in healthy Korean male volunteers by population PK modeling analysis implemented using Nonlinear Mixed Effects Modeling software. A 2×2 crossover study comparing multiple oral doses of IR and SR formulations of cilostazol were conducted. Serial plasma concentrations of cilostazol and its active metabolites, as measured by validated liquid chromatography-tandem mass spectrometry method of the IR formulation, were used in this analysis. The respective 768 plasma concentrations of cilostazol and two metabolites over time were best depicted by one compartment model, with absorption kinetics of cilostazol having mixed first- and zero-order kinetics with a time delay at the beginning of absorption. The introduction of interoccasion variabilities into D1 (duration of zero-order absorption), Ka (first order absorption rate constant), and F1 (relative bioavailability) significantly improved the model fit, and total body water was identified as a significant covariate positively affecting the clearance of cilostazol. The goodness of fit and visual predictive check plots suggested that the model constructed in this study predicted the plasma concentration of cilostazol and its two active metabolites reasonably well. The PK model we developed explored the PK characteristics of cilostazol in Korean male subjects, and may be useful for identifying optimal individual dosing regimens of cilostazol.

APPENDIX

NONMEM code

```
$PROBLEM Cilostazole_Parent_Metabolite_Model
$INPUT ID TIME DOS AMT RATE CONC DV CMT NTIM MDV PRD OCC DR GRP AGE WT HT
BMI BFM FFM TBW SLM SMM BFAT VFA ICW ECW PROT MNL CYP3A5 CYP2C19
$DATA data.csv IGNORE=@
$SUBS ADVAN13 TRANS1 TOL=5
$MODEL NCOMP=4
 COMP = (DEPOT, DEFDOSE)
 COMP = (CENTRAL)
 COMP = (M1)
 COMP = (M2)

$PK

 IOV1    = 0
 IOV2    = 0
 IOV3    = 0
 IOV4    = 0
 IF(OCC.EQ.1) IOV1 = 1
 IF(OCC.EQ.2) IOV2 = 1
 IF(OCC.EQ.3) IOV3 = 1
 IF(OCC.EQ.4) IOV4 = 1

 TVCL20 = THETA(1) *((TBW/40)**THETA(8))
 TVV2   = THETA(2)
```

```
 TVKA   = THETA(3)
 TVD1   = THETA(6)
 TVALAG1 = THETA(7)

TVCL30 = THETA(9)
TVCL40 = THETA(10)

 CL20   = TVCL20 * EXP(ETA(1))
 V2     = TVV2 * EXP(ETA(2))
 KA     = TVKA * EXP(ETA(3) * IOV1 + ETA(4) * IOV2 + ETA(5) * IOV3 + ETA(6) * IOV4)
 D1     = TVD1 * EXP(ETA(7) * IOV1 + ETA(8) * IOV2 + ETA(9) * IOV3 + ETA(10) * IOV4)
 F1     = 1    * EXP(ETA(11) * IOV1 + ETA(12) * IOV2 + ETA(13) * IOV3 + ETA(14) * IOV4)
 ALAG1            = TVALAG1*EXP(ETA(15))

 CL30 = TVCL30 * EXP(ETA(16))
 CL40 = TVCL40 * EXP(ETA(17))

FM1F = THETA(11) + ETA(18)
FM2F = THETA(12) + ETA(19)
FM1  = EXP(FM1F)/(1+EXP(FM1F)+EXP(FM2F))
FM2  = EXP(FM2F)/(1+EXP(FM1F)+EXP(FM2F))

 V3     = TVV2
 V4     = TVV2

 S2     = V2
 S3     = V3
```

```
 S4     = V4

 K20    = CL20/V2
 K30    = CL30/V3
 K40    = CL40/V4

$DES
 DADT(1) = -A(1)*KA
 DADT(2) =  A(1)*KA - A(2)*K20
 DADT(3) =  FM1*A(2)*K20 - A(3)*K30
 DADT(4) =  FM2*A(2)*K20 - A(4)*K40

$ERROR
 IPRED = F

 W1     = SQRT(THETA(4)**2 + THETA(5)**2*IPRED**2)
 W2     = SQRT(THETA(13)**2 + THETA(14)**2*IPRED**2)
 W3     = SQRT(THETA(15)**2 + THETA(16)**2*IPRED**2)

 IRES  = IPRED-DV

 Q1 = 0
 IF (CMT.EQ.2) Q1 = 1
 Y1 = IPRED + W1*ERR(1)

 Q2 = 0
 IF (CMT.EQ.3) Q2 = 1
```

```
 Y2 = IPRED + W2*ERR(2)


 Q3 = 0
 IF (CMT.EQ.4) Q3 = 1
 Y3 = IPRED + W3*ERR(3)
 Y     = Q1*Y1 + Q2*Y2 + Q3*Y3

;------INITIAL ESTIMATES - THETA-----------------------

$THETA
 7.17     FIX                    ;1   CL20 (l/h)
 9.39     FIX                    ;2   V2  (l)
 1.59E-01 FIX                    ;3   KA (h-1)
 0.000001 FIX                    ;4,  P, additive error
 2.55E-01 FIX                    ;5,  P, proportional error
 2.37     FIX                    ;6,  D1
 2.23E-01 FIX                    ;7,  ALAG1
 1.42    FIX                     ;8
;-----------------------------------------------
 (0, 2.3)                ;9   CL30 (l/h)
 (0, 7)                  ;10   CL40 (l/h)
 (-2)                    ;11  FM23
 (-2)                    ;12  FM24
 (0, 0.014)              ;13  M1  additive error
 (0, 0.13)               ;14  M1  aproportional error
 (0, 0.01)               ;15  M2  additive error
 (0, 0.16)               ;16  M2  aproportional error
```

```
;-----INITIAL ESTIMATES - OMEGA-------------------------

$OMEGA 3.42E-02  FIX
            8.66E-02  FIX

$OMEGA BLOCK(1) 8.38E-02 FIX
$OMEGA BLOCK(1) SAME
$OMEGA BLOCK(1) SAME
$OMEGA BLOCK(1) SAME

$OMEGA BLOCK(1) 7.70E-01  FIX
$OMEGA BLOCK(1) SAME
$OMEGA BLOCK(1) SAME
$OMEGA BLOCK(1) SAME

$OMEGA BLOCK(1) 1.32E-01 FIX
$OMEGA BLOCK(1) SAME
$OMEGA BLOCK(1) SAME
$OMEGA BLOCK(1) SAME
$OMEGA 3.54E-01 FIX

$OMEGA  0.06
$OMEGA  0.05
$OMEGA  0.1
$OMEGA  0.1
```

```
$SIGMA 1 FIX

$SIGMA 1 FIX

$SIGMA 1 FIX


$ESTIMATION SORT MAXEVAL=9999 PRINT=2 METHOD=COND INTER

            SLOW MSFO=335007.MSF

$COVARIANCE PRINT=E MATRIX=S

$TABLE ID TIME MDV IPRED CWRES CMT OCC CL20 V2 KA D1

        FILE=335007.FIT NOPRINT ONEHEADER

$TABLE ID CMT PRD GRP AGE WT HT BMI TBW

        ETA(1) ETA(2) ETA(3) ETA(4) ETA(5) ETA(7) ETA(8) ETA(9) ETA(10) ETA(11)

        ETA(12) ETA(13) ETA(14) ETA(15)

        FILE=335007.PAR NOPRINT ONEHEADER FIRSTONLY NOAPPEND

$TABLE ID TIME OCC CL20 V2 KA D1 ALAG1

       FILE=335007.IPK NOPRINT ONEHEADER NOAPPEND
```

Individual VPC plots of cilostazol for the final population PK model

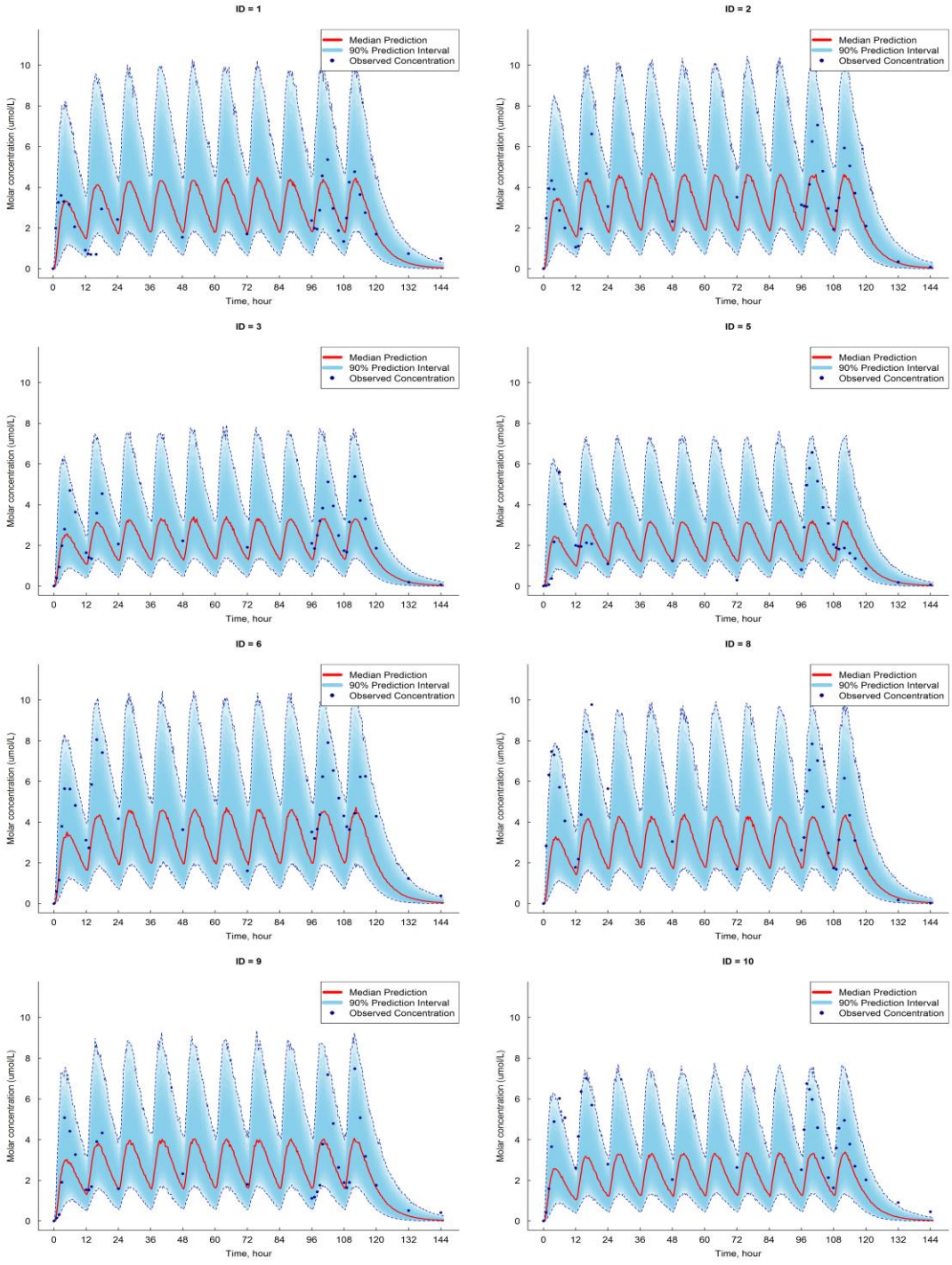

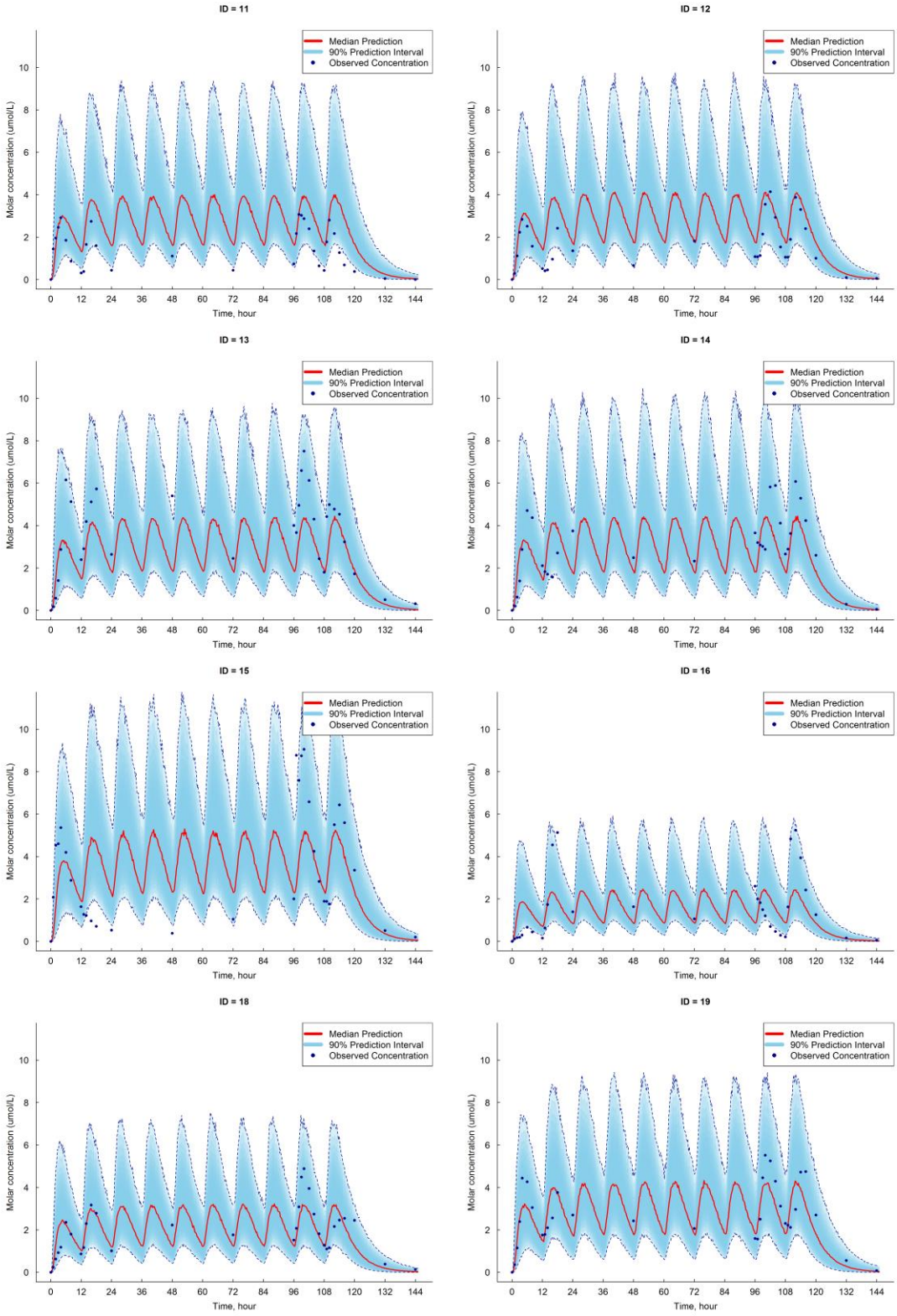
ID = 11
ID = 12
ID = 13
ID = 14
ID = 15
ID = 16
ID = 18
ID = 19
Median Prediction
90% Prediction Interval
Observed Concentration
Molar concentration (umol/L)
Time, hour

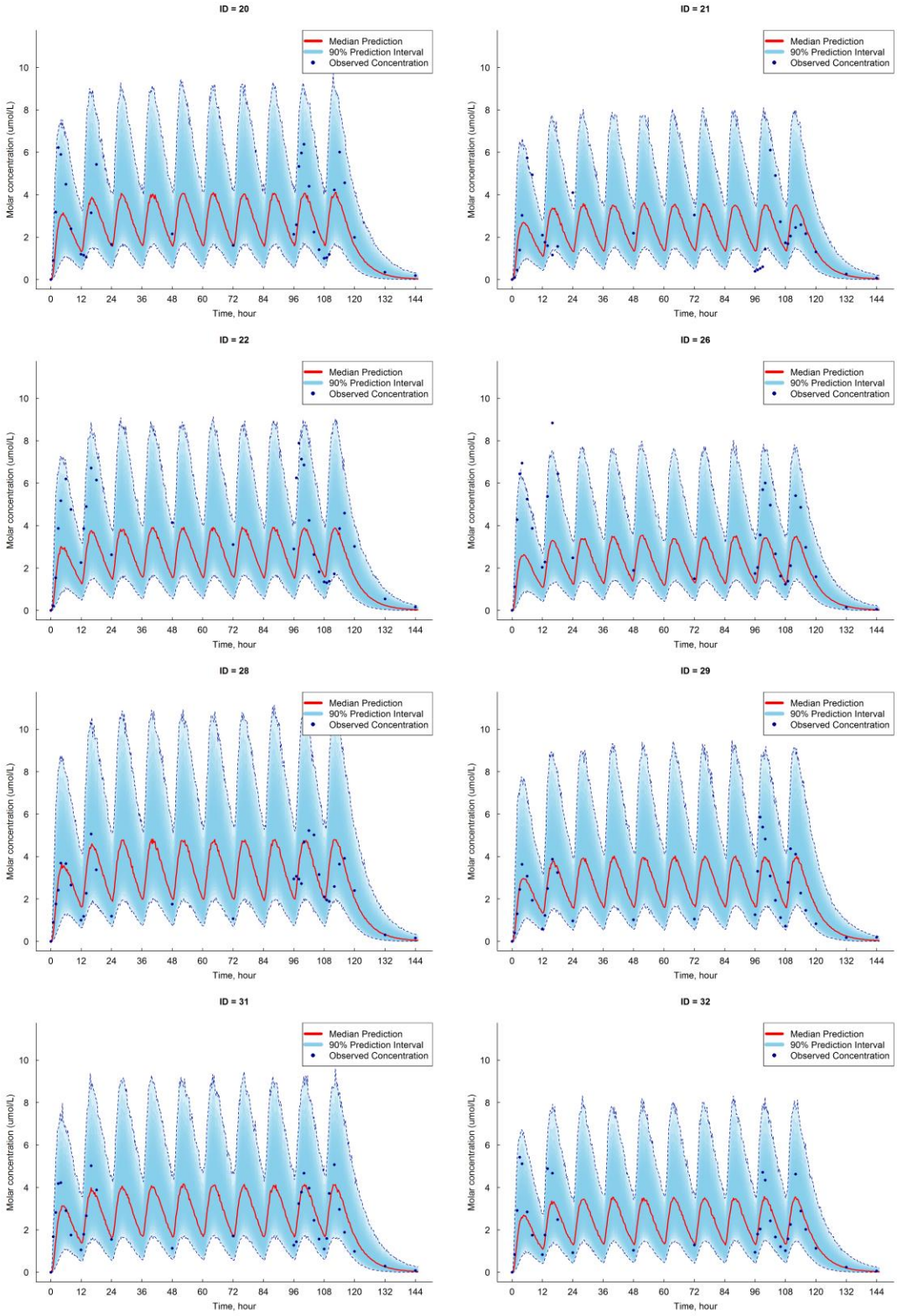
ID = 20
ID = 21
ID = 22
ID = 26
ID = 28
ID = 29
ID = 31
ID = 32
Median Prediction
90% Prediction Interval
Observed Concentration
Molar concentration (umol/L)
Time, hour
0
2
4
6
8
10
0
12
24
36
48
60
72
84
96
108
120
132
144